Microscopic View of Nucleation on Surfaces

Harald Brune, Holger Röder, Corrado Boragno, and Klaus Kern
Institut de Physique Expérimentale, Ecole Polytechnique Fédérale de Lausanne, CH-1015 Lausanne, Switzerland
(Received 23 February 1994)

Nucleation has been studied on atomic scale for Ag deposition on a Pt(111) surface at low temperature (50–120 K) by means of variable-temperature scanning tunneling microscopy. From island density versus coverage data, the transition from the initial steps of nucleation to growth and coalescence has been studied as a function of temperature. The data show that dimers are stable nuclei for $T \leq 110$ K, which facilitates quantitative comparison with rate equations from nucleation theory. The migration barrier $E_m = 157 \pm 10$ meV is determined for Ag adatoms on Pt(111) and compared with theoretical values.

PACS numbers: 68.55.–a, 61.16.Ch, 61.50.Cj, 68.35.Fx

A detailed understanding of film growth, which allows predictions not only of the thermodynamic growth mode but also of nonequilibrium kinetic morphologies, requires the study of the microscopic processes involved in epitaxy [1–3]. For the submonolayer regime these processes include the adsorption from the vapor phase and the subsequent diffusion of the adatoms on the substrate surface. This is followed by nucleation, i.e., the formation of unstable aggregates (subcritical and critical ones), which might either dissociate, or, for the critical ones, grow to stable islands upon incorporation of one extra atom. These islands then grow until coalescence sets in.

Nucleation has been a topic of current interest for theory and experiment [4,5]. Experimental studies have typically applied electron microscopy (EM) to monitor the island density versus coverage as a function of temperature and deposition flux. The results have served as a rather valid guide for the development of nucleation theory [5]. However, most of the EM studies have been carried out *ex situ* and were restricted to relatively low island densities and temperatures above 300 K.

At these temperatures, the description of nucleation becomes more complicated due to the increasing number of atomic processes involved. For example, the adsorption energy may play a role, and assumptions need to be made about various cluster binding (dissociation) energies [5]. In addition, at high substrate temperatures, island densities are low so that surface defects such as steps may appear with comparable density. As a consequence the initial atomic steps of nucleation could not be followed directly by EM. Recent scanning tunneling microscopy (STM) studies, on the other hand, have shown the importance of local effects in thin metal film growth, but they were restricted to temperatures around and above room temperature [6–11]. Thus they deal with big islands, where nucleation has already been terminated, and monitor their growth and size distribution or shape rather than focus on the nucleation process itself.

This, however, is the topic of the present Letter, where we apply variable temperature STM to study the nucleation of Ag on a Pt(111) surface on an atomic scale at temperatures between 50 and 120 K. The low temperatures allow deduction of kinetic parameters as the Ag migration barrier with high precision. It turns out that at these temperatures dimers are the stable nuclei. This reduces a nucleation event to the encounter of two diffusing atoms and thus allows for direct quantitative comparison with simple rate equations from nucleation theory.

The experiments were performed with a variable-temperature STM (25–600 K) operating in UHV [12]. The Ag submonolayers (purity 99.995%) were evaporated with a molecular beam epitaxy Knudsen cell at a background pressure better than 2.0×10^{-10} mbar. The deposition flux was set to $R = 1.1 \times 10^{-3}$ ML/s [1 ML (monolayer) corresponds to the Pt(111) atom density of 1.50×10^{15} cm^{-2}]. STM images were measured isothermally after deposition. All images shown here were taken in differential mode. Island densities are given in islands per Pt substrate atom, i.e., in ML. They have been evaluated exclusively on terrace areas far enough separated from steps (more than the mean island distance) to avoid errors caused by their presence. They were corrected for lateral drift by considering the drift vector of consecutive images.

In order to study nucleation it is convenient to follow the evolution of the submonolayer film morphology with increasing coverage, i.e., the development of the island density, size, and shape. This is shown in Figs. 1(a) and 1(b) for deposition of Ag onto the Pt(111) surface held at 50 K for coverages of 0.007 and 0.12 ML, respectively. Ag islands are imaged as bright dots (of height 2.9 Å in absolute STM topographs) which are randomly distributed over the surface. It is evident that the island density has increased from Fig. 1(a) to 1(b) as had the coverage. Quantitatively, the island density can be obtained from STM images simply by island counting and dividing by the area of the image. The quotient of coverage and island density is then the average island size. In Fig. 1(a), it was found to be 1.6 ± 0.6 atoms per island and in Fig. 1(b), 2.8 ± 0.4 atoms per island. Therefore the STM images Figs. 1(a) and 1(b) show that there are mostly dimers which form upon deposition of Ag at 50 K. (Because

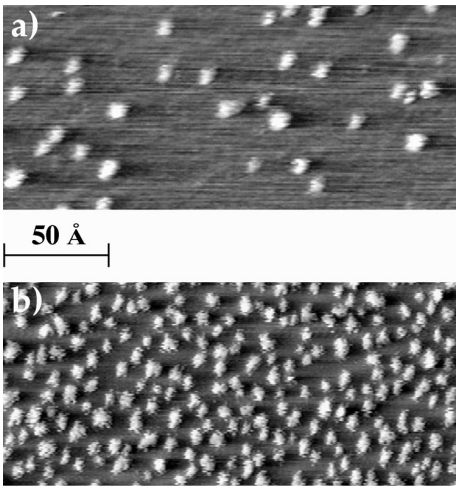

FIG. 1. STM images of 0.7% (a) and 12% (b) of a monolayer silver deposited on Pt(111) at 50 K. Mostly dimers are formed under these conditions. [(a) island density $\rho = (4.4 \pm 0.7) \times 10^{-3}$ ML; (b) $\rho = (4.2 \pm 0.5) \times 10^{-2}$ ML.]

of the curvature of the tip these dimers do not appear in their atomic structure but as round dots.) The increase of the coverage by a factor of 17 from Fig. 1(a) to 1(b) corresponds quite closely to a factor of 10 increase in island density. Thus we are in the coverage regime of nucleation. In this regime, diffusing Ag atoms find with a higher probability a second mobile partner to create a new nucleus than to attach to an existing island. (The island density does not increase proportionally with coverage because at the higher coverage partial growth occurs.) On the other hand, these images show that dimers are stable at 50 K, therefore the critical nucleus is a single atom.

In general, the size of the critical nucleus can be deduced from STM data by dividing the coverage by the island density at the coverage regime of pure nucleation. Values of island densities versus coverage are shown in a logarithmic plot in Fig. 2 for various temperatures. For 50 and 60 K, the island densities show a linear increase up to the highest coverage investigated. This implies that at these temperatures, for coverages up to 0.1 ML, nucleation is not yet terminated. The average size of these islands is approximately 2 Ag atoms (as can be seen from comparison with the dashed line). At 75 K, on the other hand, the data show that saturation sets in at 0.6% of a monolayer; at 80 K saturation occurs at coverages below 0.5% of a ML.

The island density over the complete coverage regime from nucleation to growth was monitored at 75 K. Four STM images are shown in Figs. 3(a) to 3(d) in order to illustrate how the island density as well as their shape changes from nucleation to growth. In Figs. 3(a) and 3(b), it is seen that, on the average, the islands are still dimers [mean size 2.4 ± 0.4 atoms and 2.6 ± 0.5 atoms for Figs. 3(a) and 3(b), respectively], which means that they show the nucleation regime. Figure 3(c), however,

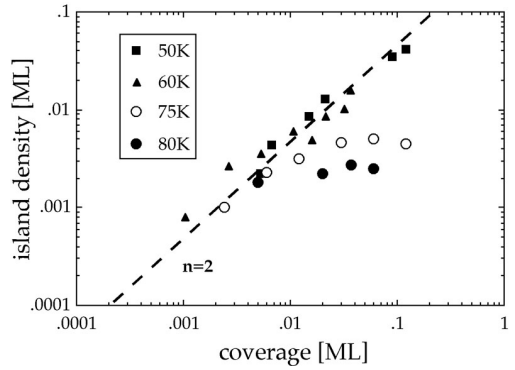

FIG. 2. Island density versus coverage as deduced from STM measurements performed at 50, 60, 75, and 80 K.

demonstrates the transition from nucleation to growth. Θ was increased by a factor of 5 with respect to Fig. 3(b), which resulted in an increase in density by a factor of only 2 accompanied by an increase in the average island size to 6.4 ± 1.1 atoms. Further increase of the coverage by a factor of 2 leads to exclusive island growth [11.9 ± 2.0 atoms per island see Fig. 3(d)]. As can be seen from Fig. 3(d), island growth leads to (anisotropic) branching of the islands, caused by the low perimeter mobility for

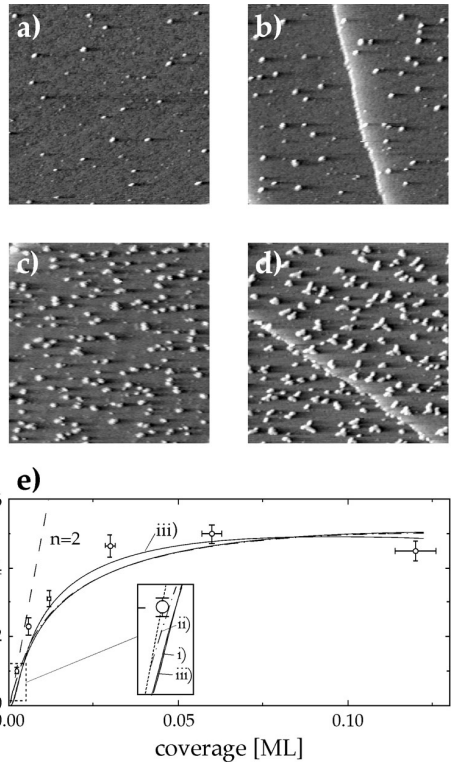

FIG. 3. Four STM images showing the evolution of the island shape and density as a function of coverage at 75 K (a) coverage Θ = 0.24%, $\rho = 0.10\%$, (b) Θ = 0.60%, $\rho = 0.23\%$, (c) Θ = 3.0%, $\rho = 0.46\%$, (d) Θ = 6.0%, $\rho = 0.50\%$ of 1 ML [(a)–(d) all with 420 × 420 Å], (e) STM data (dots) and calculated curves of island density versus coverage for deposition at 75 K with $R = 1.1 \times 10^{-3}$ ML s^{-1}.

attaching atoms [13,14]. Note that this branching is not observed in Fig. 3(c), which implies that it proceeds only if the islands have reached a certain size, which we have determined to be the heptamer.

A linear plot of the island density versus coverage is shown in Fig. 3(e). The STM data are represented by dots with error bars, while calculated curves show results from integrated rate equations as discussed below. For coverages below 0.006 ML, the densities (the first two data points) are on the initial slope of 0.5, indicating an average nucleus size of 2 (see dashed line). Above this coverage the gradual transition from nucleation to growth takes place up to 0.030 ML. At higher coverages, saturation sets in and island growth predominantly occurs. At this stage existing islands are dense enough that each arriving Ag atom has sufficient mobility to reach them with a higher probability than to hit a second mobile atom and to form a new nucleus.

The saturation island density thus contains direct information about the Ag adatom diffusion and should follow an Arrhenius law [5]. Saturation island densities versus temperature are shown in Fig. 4 for the range from 65 to 120 K. Between 65 K and 110 K the saturation island densities lie on a straight line in the Arrhenius representation. This behavior allows one to determine rather precisely the migration barrier for Ag adatom diffusion on Pt(111) [see the range of T^{-1}, which is 6×10^{-3} K^{-1} compared to only $(1-2) \times 10^{-3}$ K^{-1} for typical EM studies].

The data in Fig. 2 showed that for temperatures between 50 and 80 K dimers are the stable nuclei. From annealing experiments [2] it turned out that dimers are indeed stable up to 110 K; only above this temperature the onset of diffusion and/or dissociation of Ag dimers was observed. It is therefore concluded that for temperatures below 110 K in Fig. 4 dimers are stable, and monomers are the critical nuclei. In this temperature range, Eq. (2.15) in Ref. [5] can thus be applied in its simplest form, which is valid for complete condensation (reevaporation can be excluded at low temperature), for 2D islands and a critical nucleus size of 1. For this case it reads $n_s(T) \propto (R\nu_0)^{1/3} \exp(E_m/3kT)$. From the slope of the line that fits the STM data ($65 \leq T \leq 110$ K) a migration barrier of $E_m = 157 \pm 10$ meV is obtained. The substantial deviation of the measured saturation island density at 120 K from the "dimer fit" marks the transition to the nucleation regime with trimers as stable nuclei.

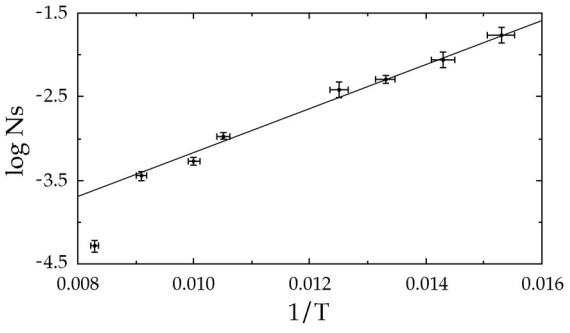

FIG. 4. Arrhenius plot of saturation island densities derived from STM for 65 to 120 K.

The migration barrier of 157 meV is a rather reasonable value for diffusion of metal atoms on close packed metal surfaces. Values of 156 ± 22, 300, 269 ± 4, and 150 ± 100 meV have been obtained experimentally for self-diffusion on (111) surfaces of the fcc metals Rh, Ni, Ir [1], and Ag [15], respectively. For Ag/Pt(111) recent first-principles local-density-functional calculations [16] obtained a diffusion barrier of 200 meV, rather close to the value derived from our study, whereas a much smaller value of 58 ± 3 meV has been obtained in an embedded-atom calculation [17]. The Ag-Ag binding energy on Pt(111) can be estimated to 320 ± 20 meV from the temperature of 120 K at which dimer dissociation becomes detectable at the time scale of the experiment (assuming $\nu_0 = 1 \times 10^{12}$ s^{-1}). This compares well to the values obtained for Ag on Ag(111) (0.25 ± 0.05 eV experiment, 0.28 eV theory) [15], 0.18 eV has been calculated for Ag/Pt(111) [17].

In the following we will discuss the rate equations of nucleation and compare the results obtained by their numerical integration with experiment for the case of 75 K, as shown in Fig. 3(e). The differential equations of nucleation, in our simple case where dimers are stable and reevaporation, as well as dimer migration does not occur, are the following:

$$\frac{dn_1}{dt} = R - 2\sigma_1 D n_1^2 - \sigma_x D n_1 n_x - R(Rt - n_1), \quad (1)$$

$$\frac{dn_x}{dt} = \sigma_1 D n_1^2 - 2n_x \times [2\sigma_1 D n_1^2 + \sigma_x D n_1 n_x + R(Rt - n_1)]. \quad (2)$$

The terms in Eq. (1) describe the increase of the density of monomers due to the flux R, their decrease due to the encounter of two diffusing atoms under creation of a dimer and disappearance of the two atoms, the decrease occurring when a monomer is captured by a stable island, and that caused by atoms impinging on top of stable islands. In Eq. (2) the first term is the increase of density of stable islands n_x due to creation of dimers, whereas the second term in brackets represents its decrease due to coalescence [see Eqs. (2.8), (2.9), and (2.11) in [5]]. The diffusion is given as $D = \frac{1}{4}\nu_0 \exp(-E_m/kT)$ in unit cells per second. The lower curve in Fig. 3(e), labeled (i), shows the evolution of n_x as obtained from integrating Eqs. (1) and (2) for Ag deposition onto the Pt(111) surface at 75 K with the flux used in the experiments. The migration barrier of $E_m = 0.157$ eV derived from our STM data was used for the calculation. The attempt frequency has been set to $\nu_0 = 1.7 \times 10^{13}$ s^{-1} in order to achieve the experimental saturation value for the island density (from Fig. 4, $1 \times 10^{13} \leq \nu_0 \leq 4 \times 10^{14}$ s^{-1} is inferred).

For curve (i), the capture rates σ were interpreted in an atomistic model as cross sections for capture of diffusing

atoms by islands or atoms. Their size dependence was empirically determined to be $\sigma(n):=2 + n^{1/1.7}$, where n is the island size in number of atoms. Therefore monomers have $\sigma_1 = 3$ which comes from the fact that besides central impact also atoms approaching each other to one nearest neighbor distance are trapped. The cross section increases as the 1.7th root of island size rather than the square root due to the fractal character of the islands [13]. Accordingly in Eqs. (1) and (2), σ_x has been taken to be dependent on the average island size which is given by $n = (Rt - n_1)/n_x$. The model simplifies the physical picture in so far as it assumes a homogeneous distribution of mobile monomers, which are then either trapped on their own or at condensed islands. However, it reproduces quite well the main features of the experiment. Curve (i) of Fig. 3(e) has an initial slope of 0.5, and it shows the gradual transition from nucleation to growth. We note that this coincidence with experiment cannot be achieved if constant values for σ_x are used, hence the size dependence of σ_x is essential.

Compared to the experiment, however, curve (i) has a curvature which is too small. At the transition from nucleation to growth (0.01–0.03 ML) it lies below the experimental data and at the onset of coalescence, which was found between 0.06 and 0.12 ML, curve (i) continues to increase. The density of diffusing monomers has been assumed to be isotropic for the calculation. Actually, it decreases at the island edges due to capture there. For the calculated curve (iii) [upper curve in Fig. 3(e)] we took this into account and interpreted the capture rates in the "classical" sense as the gradient of the monomer concentration at the island edges. These gradients were obtained by solving a 2D diffusion equation in lattice approximation [18]. At the onset of nucleation curve (iii) overlaps with curve (i). However, it raises more steeply and saturates earlier than curve (i) and thus shows better agreement with experiment.

For the very low coverages, it should be emphasized that this calculation gives the island densities during deposition, whereas the STM experiment samples the distribution a few minutes after deposition. We therefore calculated how the system develops if the flux is interrupted at given coverages and one waits until the island densities have reached their equilibrium value. At 75 K the system equilibrates in less than 10 s, and, we therefore image this equilibrium state with STM. The calculated equilibrium density of stable islands n_x, which had developed 20 s after interrupting the flux, is shown in the dash-dotted curve (ii) as a function of coverage. For this calculation, the choice between capture rates is of no importance because curves (i) and (iii) overlap at low coverages. Thus for simplicity, σ_x has been defined as in curve (i). Equilibration leads, for the smallest coverages, to a slightly higher island density, due to the initially high density of monomers which predominantly create new islands after the flux is interrupted. Correspondingly, curve (ii) is closer to the experiment for the very beginning of deposition. For coverages higher than 0.006 ML, however, it is seen that the island density imaged by STM is exactly that present during deposition [curves (i) and (ii) are in coincidence]. This is due to the fact that, at coverages of 0.006 ML and higher, monomers remaining after deposition predominantly attach to existing islands rather than create new ones.

The fact that the STM experiments show no difference in the densities obtained during deposition, at least for saturation, in the whole temperature range addressed in 4, is important to note. This is the condition to extract diffusion constants from saturation island densities, because the flux is the only parameter introducing time. (Note that the expected relation $n_s \propto R^{1/3}$ has been confirmed in the present experiment.)

In conclusion, the STM data presented here reveal the first confirmation of nucleation theory for the low temperature regime where the influence of kinetics on the atomic processes involved in film growth is most pronounced. The initial steps of nucleation as well as island growth and coalescence could be followed on an atomic scale. It has been shown that dimers are the stable nuclei which allowed us to deduce the kinetic parameters of Ag adatom diffusion on Pt(111) as well as quantitative comparison with rate equations from nucleation theory. Integrating these rate equations yields quantitative agreement with experiment for coverages from pure nucleation to the onset of coalescence.

We gratefully acknowledge discussions with A. Zangwill.

[1] G. Ehrlich, Surf. Sci. **246**, 1 (1991).
[2] H. Röder *et al.*, Nature **366**, 141 (1993).
[3] S.C. Wang and G. Ehrlich, Phys. Rev. Lett. **71**, 4174 (1993).
[4] B. Lewis and J.C. Anderson, *Nucleation and Growth of Thin Films* (Academic Press, New York, 1978).
[5] J.A. Venables, G.D.T. Spiller, and M. Hanbücken, Rep. Prog. Phys. **47**, 399 (1984).
[6] J.A. Stroscio, D.T. Pierce, and R.A. Dragoset, Phys. Rev. Lett. **70**, 3615 (1993).
[7] J.A. Stroscio and D.T. Pierce, Phys. Rev. B **49**, 8522 (1994).
[8] C. Günther *et al.*, Ber. Bunsen-Ges. Phys. Chem. **97**, 522 (1993).
[9] S. Günther *et al.*, Phys. Rev. Lett. **72**, 553 (1994).
[10] T. Michely *et al.*, Phys. Rev. Lett. **70**, 3943 (1993); Surf. Sci. **272**, 161 (1992).
[11] P.A. Bennett, S.A. Parikh, and D.G. Cahill, J. Vac. Sci. Technol. A **11**, 1680 (1993).
[12] H. Röder *et al.*, Surf. Sci. **298**, 121 (1993).
[13] H. Brune *et al.*, Nature **369**, 469 (1994).
[14] T.A. Witten and L.M. Sander, Phys. Rev. B **27**, 5686 (1983).
[15] G.W. Jones *et al.*, Phys. Rev. Lett. **65**, 3317 (1990).
[16] P.J. Feibelman, Surf. Sci. **313**, L801 (1994).
[17] P. Blandin and C. Massobrio, Surf. Sci. **279**, L219 (1992).
[18] J.A. Venables, Philos. Mag. **17**, 697 (1973).